

University of Nebraska - Lincoln

DigitalCommons@University of Nebraska - Lincoln

Kenneth Bloom Publications

Research Papers in Physics and Astronomy

12-31-2002

Limits on Extra Dimensions and New Particle Production in the Exclusive Photon

Darin Acosta

University of Florida, acosta@phys.ufl.edu

Kenneth A. Bloom

University of Nebraska - Lincoln, kbloom2@unl.edu

Collider Detector at Fermilab Collaboration

Follow this and additional works at: <http://digitalcommons.unl.edu/physicsbloom>



Part of the [Physics Commons](#)

Acosta, Darin; Bloom, Kenneth A.; and Fermilab Collaboration, Collider Detector at, "Limits on Extra Dimensions and New Particle Production in the Exclusive Photon" (2002). *Kenneth Bloom Publications*. 59.

<http://digitalcommons.unl.edu/physicsbloom/59>

This Article is brought to you for free and open access by the Research Papers in Physics and Astronomy at DigitalCommons@University of Nebraska - Lincoln. It has been accepted for inclusion in Kenneth Bloom Publications by an authorized administrator of DigitalCommons@University of Nebraska - Lincoln.

Limits on Extra Dimensions and New Particle Production in the Exclusive Photon and Missing Energy Signature in $p\bar{p}$ Collisions at $\sqrt{s} = 1.8$ TeV

D. Acosta,¹³ T. Affolder,²⁴ H. Akimoto,⁴⁷ M. G. Albrow,¹² D. Ambrose,³⁴ D. Amidei,²⁶ K. Anikeev,²⁵ J. Antos,¹ G. Apollinari,¹² T. Arisawa,⁴⁷ A. Artikov,¹⁰ T. Asakawa,⁴⁵ W. Ashmanskas,⁹ F. Afzar,³² P. Azzi-Bacchetta,³³ N. Bacchetta,³³ H. Bachacou,²⁴ W. Badgett,¹² S. Bailey,¹⁷ P. de Barbaro,³⁸ A. Barbaro-Galtieri,²⁴ V. E. Barnes,³⁷ B. A. Barnett,²⁰ S. Baroiant,⁵ M. Barone,¹⁴ G. Bauer,²⁵ F. Bedeschi,³⁵ S. Behari,²⁰ S. Belforte,⁴⁴ W. H. Bell,¹⁶ G. Bellettini,³⁵ J. Bellinger,⁴⁸ D. Benjamin,¹¹ J. Bensinger,⁴ A. Beretvas,¹² J. Berryhill,⁹ A. Bhatti,³⁹ M. Binkley,¹² D. Bisello,³³ M. Bishai,¹² R. E. Blair,² C. Blocker,⁴ K. Bloom,²⁶ B. Blumenfeld,²⁰ S. R. Blusk,³⁸ A. Bocci,³⁹ A. Bodek,³⁸ G. Bolla,³⁷ Y. Bonushkin,⁶ D. Bortoletto,³⁷ J. Boudreau,³⁶ A. Brandl,²⁸ C. Bromberg,²⁷ M. Brozovic,¹¹ E. Brubaker,²⁴ N. Bruner,²⁸ J. Budagov,¹⁰ H. S. Budd,³⁸ K. Burkett,¹⁷ G. Busetto,³³ K. L. Byrum,² S. Cabrera,¹¹ P. Calafiura,²⁴ M. Campbell,²⁶ W. Carithers,²⁴ J. Carlson,²⁶ D. Carlsmith,⁴⁸ W. Caskey,⁵ A. Castro,³ D. Cauz,⁴⁴ A. Cerri,³⁵ A. W. Chan,¹ P. S. Chang,¹ P. T. Chang,¹ J. Chapman,²⁶ C. Chen,³⁴ Y. C. Chen,¹ M. -T. Cheng,¹ M. Chertok,⁵ G. Chiarelli,³⁵ I. Chirikov-Zorin,¹⁰ G. Chlachidze,¹⁰ F. Chlebana,¹² L. Christofek,¹⁹ M. L. Chu,¹ J. Y. Chung,³⁰ W. -H. Chung,⁴⁸ Y. S. Chung,³⁸ C. I. Ciobanu,³⁰ A. G. Clark,¹⁵ M. Coca,³⁸ A. P. Colijn,¹² A. Connolly,²⁴ M. Convery,³⁹ J. Conway,⁴⁰ M. Cordelli,¹⁴ J. Cranshaw,⁴² R. Culbertson,¹² D. Dagenhart,⁴⁶ S. D'Auria,¹⁶ F. DeJongh,¹² S. Dell'Agnello,¹⁴ M. Dell'Orso,³⁵ S. Demers,³⁸ L. Demortier,³⁹ M. Deninno,³ P. F. Derwent,¹² T. Devlin,⁴⁰ J. R. Dittmann,¹² A. Dominguez,²⁴ S. Donati,³⁵ M. D'Onofrio,³⁵ T. Dorigo,¹⁷ I. Dunietz,¹² N. Eddy,¹⁹ K. Einsweiler,²⁴ E. Engels, Jr.,³⁶ R. Erbacher,¹² D. Errede,¹⁹ S. Errede,¹⁹ Q. Fan,³⁸ H.-C. Fang,²⁴ R. G. Feild,⁴⁹ J. P. Fernandez,³⁷ C. Ferretti,³⁵ R. D. Field,¹³ I. Fiori,³ B. Flaughner,¹² L. R. Flores-Castillo,³⁶ G. W. Foster,¹² M. Franklin,¹⁷ J. Freeman,¹² J. Friedman,²⁵ H. J. Frisch,⁹ Y. Fukui,²³ I. Furic,²⁵ S. Galeotti,³⁵ A. Gallas,²⁹ M. Gallinaro,³⁹ T. Gao,³⁴ M. Garcia-Sciveres,²⁴ A. F. Garfinkel,³⁷ P. Gatti,³³ C. Gay,⁴⁹ D. W. Gerdes,²⁶ E. Gerstein,⁸ P. Giannetti,³⁵ K. Giolo,³⁷ M. Giordani,⁵ P. Giromini,¹⁴ V. Glagolev,¹⁰ D. Glenzinski,¹² M. Gold,²⁸ J. Goldstein,¹² G. Gomez,⁷ I. Gorelov,²⁸ A. T. Goshaw,¹¹ Y. Gotra,³⁶ K. Goulianos,³⁹ C. Green,³⁷ G. Grim,⁵ C. Grosso-Pilcher,⁹ M. Guenther,³⁷ G. Guillian,²⁶ J. Guimaraes da Costa,¹⁷ R. M. Haas,¹³ C. Haber,²⁴ S. R. Hahn,¹² C. Hall,¹⁷ T. Handa,¹⁸ R. Handler,⁴⁸ F. Happacher,¹⁴ K. Hara,⁴⁵ A. D. Hardman,³⁷ R. M. Harris,¹² F. Hartmann,²¹ K. Hatakeyama,³⁹ J. Hauser,⁶ J. Heinrich,³⁴ A. Heiss,²¹ M. Herndon,²⁰ C. Hill,⁵ A. Hocker,³⁸ K. D. Hoffman,⁹ R. Hollebeek,³⁴ L. Holloway,¹⁹ B. T. Huffman,³² R. Hughes,³⁰ J. Huston,²⁷ J. Huth,¹⁷ H. Ikeda,⁴⁵ J. Incandela,^{12,*} G. Introzzi,³⁵ A. Ivanov,³⁸ J. Iwai,⁴⁷ Y. Iwata,¹⁸ E. James,²⁶ M. Jones,³⁴ U. Joshi,¹² H. Kambara,¹⁵ T. Kamon,⁴¹ T. Kaneko,⁴⁵ M. Karagoz Unel,²⁹ K. Karr,⁴⁶ S. Kartal,¹² H. Kasha,⁴⁹ Y. Kato,³¹ T. A. Keaffaber,³⁷ K. Kelley,²⁵ M. Kelly,²⁶ R. D. Kennedy,¹² R. Kephart,¹² D. Khazins,¹¹ T. Kikuchi,⁴⁵ B. Kilminster,³⁸ B. J. Kim,²² D. H. Kim,²² H. S. Kim,¹⁹ M. J. Kim,⁸ S. B. Kim,²² S. H. Kim,⁴⁵ Y. K. Kim,²⁴ M. Kirby,¹¹ M. Kirk,⁴ L. Kirsch,⁴ S. Klimenko,¹³ P. Koehn,³⁰ K. Kondo,⁴⁷ J. Konigsberg,¹³ A. Korn,²⁵ A. Korytov,¹³ E. Kovacs,² J. Kroll,³⁴ M. Kruse,¹¹ V. Krutelyov,⁴¹ S. E. Kuhlmann,² K. Kurino,¹⁸ T. Kuwabara,⁴⁵ A. T. Laasanen,³⁷ N. Lai,⁹ S. Lami,³⁹ S. Lammel,¹² J. Lancaster,¹¹ M. Lancaster,²⁴ R. Lander,⁵ A. Lath,⁴⁰ G. Latino,²⁸ T. LeCompte,² Y. Le,²⁰ K. Lee,⁴² S. W. Lee,⁴¹ S. Leone,³⁵ J. D. Lewis,¹² M. Lindgren,⁶ T. M. Liss,¹⁹ J. B. Liu,³⁸ T. Liu,¹² Y. C. Liu,¹ D. O. Litvintsev,¹² O. Lobban,⁴² N. S. Lockyer,³⁴ J. Loken,³² M. Loreti,³³ D. Lucchesi,³³ P. Lukens,¹² S. Lusin,⁴⁸ L. Lyons,³² J. Lys,²⁴ R. Madrak,¹⁷ K. Maeshima,¹² P. Maksimovic,²⁰ L. Malferrari,³ M. Mangano,³⁵ G. Manca,³² M. Mariotti,³³ G. Martignon,³³ M. Martin,²⁰ A. Martin,⁴⁹ V. Martin,²⁹ J. A. J. Matthews,²⁸ P. Mazzanti,³ K. S. McFarland,³⁸ P. McIntyre,⁴¹ M. Menguzzato,³³ A. Menzione,³⁵ P. Merkel,¹² C. Mesropian,³⁹ A. Meyer,¹² T. Miao,¹² R. Miller,²⁷ J. S. Miller,²⁶ H. Minato,⁴⁵ S. Miscetti,¹⁴ M. Mishina,²³ G. Mitselmakher,¹³ Y. Miyazaki,³¹ N. Moggi,³ E. Moore,²⁸ R. Moore,²⁶ Y. Morita,²³ T. Moulrik,³⁷ M. Mulhearn,²⁵ A. Mukherjee,¹² T. Muller,²¹ A. Munar,³⁵ P. Murat,¹² S. Murgia,²⁷ J. Nachtman,⁶ V. Nagaslaev,⁴² S. Nahn,⁴⁹ H. Nakada,⁴⁵ I. Nakano,¹⁸ R. Napora,²⁰ C. Nelson,¹² T. Nelson,¹² C. Neu,³⁰ D. Neuberger,²¹ C. Newman-Holmes,¹² C.-Y. P. Ngan,²⁵ T. Nigmanov,³⁶ H. Niu,⁴ L. Nodulman,² A. Nomerotski,¹³ S. H. Oh,¹¹ Y. D. Oh,²² T. Ohmoto,¹⁸ T. Ohsugi,¹⁸ R. Oishi,⁴⁵ T. Okusawa,³¹ J. Olsen,⁴⁸ P. U. E. Onyisi,⁹ W. Orejudos,²⁴ C. Pagliarone,³⁵ F. Palmonari,³⁵ R. Paoletti,³⁵ V. Papadimitriou,⁴² D. Partos,⁴ J. Patrick,¹² G. Pauletta,⁴⁴ M. Paulini,⁸ T. Pauly,³² C. Paus,²⁵ D. Pellett,⁵ L. Pescara,³³ T. J. Phillips,¹¹ G. Piacentino,³⁵ J. Piedra,⁷ K. T. Pitts,¹⁹ A. Pompos,³⁷ L. Pondrom,⁴⁸ G. Pope,³⁶ T. Pratt,³² F. Prokoshin,¹⁰ J. Proudfoot,² F. Ptohos,¹⁴ O. Pukhov,¹⁰ G. Punzi,³⁵ J. Rademacker,³² A. Rakitine,²⁵ F. Ratnikov,⁴⁰ D. Reher,²⁴ A. Reichold,³² P. Renton,³² A. Ribon,³³ W. Riegler,¹⁷ F. Rimondi,³ L. Ristori,³⁵ M. Riveline,⁴³ W. J. Robertson,¹¹ T. Rodrigo,⁷ S. Rolli,⁴⁶ L. Rosenson,²⁵ R. Roser,¹² R. Rossin,³³ C. Rott,³⁷ A. Roy,³⁷ A. Ruiz,⁷ A. Safonov,⁵ R. St. Denis,¹⁶ W. K. Sakumoto,³⁸ D. Saltzberg,⁶ C. Sanchez,³⁰ A. Sansoni,¹⁴ L. Santi,⁴⁴ H. Sato,⁴⁵ P. Savard,⁴³ A. Savoy-Navarro,¹² P. Schlabach,¹² E. E. Schmidt,¹² M. P. Schmidt,⁴⁹

M. Schmitt,²⁹ L. Scodellaro,³³ A. Scott,⁶ A. Scribano,³⁵ A. Sedov,³⁷ S. Seidel,²⁸ Y. Seiya,⁴⁵ A. Semenov,¹⁰ F. Semeria,³ T. Shah,²⁵ M. D. Shapiro,²⁴ P. F. Shepard,³⁶ T. Shibayama,⁴⁵ M. Shimojima,⁴⁵ M. Shochet,⁹ A. Sidoti,³³ J. Siegrist,²⁴ A. Sill,⁴² P. Sinervo,⁴³ P. Singh,¹⁹ A. J. Slaughter,⁴⁹ K. Sliwa,⁴⁶ F. D. Snider,¹² A. Solodsky,³⁹ J. Spalding,¹² T. Speer,¹⁵ M. Spezziga,⁴² P. Sphicas,²⁵ F. Spinella,³⁵ M. Spiropulu,⁹ L. Spiegel,¹² J. Steele,⁴⁸ A. Stefanini,³⁵ J. Strologas,¹⁹ F. Strumia,¹⁵ D. Stuart,^{12,*} K. Sumorok,²⁵ T. Suzuki,⁴⁵ T. Takano,³¹ R. Takashima,¹⁸ K. Takikawa,⁴⁵ P. Tamburello,¹¹ M. Tanaka,⁴⁵ B. Tannenbaum,⁶ M. Tecchio,²⁶ R. J. Tesarek,¹² P. K. Teng,¹ K. Terashi,³⁹ S. Tether,²⁵ A. S. Thompson,¹⁶ E. Thomson,³⁰ R. Thurman-Keup,² P. Tipton,³⁸ S. Tkaczyk,¹² D. Toback,⁴¹ K. Tollefson,²⁷ A. Tollestrup,¹² D. Tonelli,³⁵ M. Tonnesmann,²⁷ H. Toyoda,³¹ W. Trischuk,⁴³ J. F. de Troconiz,¹⁷ J. Tseng,²⁵ D. Tsybychev,¹³ N. Turini,³⁵ F. Ukegawa,⁴⁵ T. Vaiciulis,³⁸ J. Valls,⁴⁰ E. Vataha,³⁵ S. Vajcic III,¹² G. Velev,¹² G. Veramendi,²⁴ R. Vidal,¹² I. Vila,⁷ R. Vilar,⁷ I. Volobouev,²⁴ M. von der Mey,⁶ D. Vucinic,²⁵ R. G. Wagner,² R. L. Wagner,¹² W. Wagner,²¹ N. B. Wallace,⁴⁰ Z. Wan,⁴⁰ C. Wang,¹¹ M. J. Wang,¹ S. M. Wang,¹³ B. Ward,¹⁶ S. Waschke,¹⁶ T. Watanabe,⁴⁵ D. Waters,³² T. Watts,⁴⁰ M. Weber,²⁴ H. Wenzel,²¹ W. C. Wester III,¹² A. B. Wicklund,² E. Wicklund,¹² T. Wilkes,⁵ H. H. Williams,³⁴ P. Wilson,¹² B. L. Winer,³⁰ D. Winn,²⁶ S. Wolbers,¹² D. Wolinski,²⁶ J. Wolinski,²⁷ S. Wolinski,²⁶ S. Worm,⁴⁰ X. Wu,¹⁵ J. Wyss,³⁵ U. K. Yang,⁹ W. Yao,²⁴ G. P. Yeh,¹² P. Yeh,¹ K. Yi,²⁰ J. Yoh,¹² C. Yosef,²⁷ T. Yoshida,³¹ I. Yu,²² S. Yu,³⁴ Z. Yu,⁴⁹ J. C. Yun,¹² A. Zanetti,⁴⁴ F. Zetti,²⁴ and S. Zucchelli³

(CDF Collaboration)

¹*Institute of Physics, Academia Sinica, Taipei, Taiwan 11529, Republic of China*

²*Argonne National Laboratory, Argonne, Illinois 60439*

³*Istituto Nazionale di Fisica Nucleare, University of Bologna, I-40127 Bologna, Italy*

⁴*Brandeis University, Waltham, Massachusetts 02254*

⁵*University of California at Davis, Davis, California 95616*

⁶*University of California at Los Angeles, Los Angeles, California 90024*

⁷*Instituto de Fisica de Cantabria, CSIC-University of Cantabria, 39005 Santander, Spain*

⁸*Carnegie Mellon University, Pittsburgh, Pennsylvania 15218*

⁹*Enrico Fermi Institute, University of Chicago, Chicago, Illinois 60637*

¹⁰*Joint Institute for Nuclear Research, RU-141980 Dubna, Russia*

¹¹*Duke University, Durham, North Carolina 27708*

¹²*Fermi National Accelerator Laboratory, Batavia, Illinois 60510*

¹³*University of Florida, Gainesville, Florida 32611*

¹⁴*Laboratori Nazionali di Frascati, Istituto Nazionale di Fisica Nucleare, I-00044 Frascati, Italy*

¹⁵*University of Geneva, CH-1211 Geneva 4, Switzerland*

¹⁶*Glasgow University, Glasgow G12 8QQ, United Kingdom*

¹⁷*Harvard University, Cambridge, Massachusetts 02138*

¹⁸*Hiroshima University, Higashi-Hiroshima 724, Japan*

¹⁹*University of Illinois, Urbana, Illinois 61801*

²⁰*The Johns Hopkins University, Baltimore, Maryland 21218*

²¹*Institut für Experimentelle Kernphysik, Universität Karlsruhe, 76128 Karlsruhe, Germany*

²²*Center for High Energy Physics: Kyungpook National University, Taegu 702-701, Korea;*

Seoul National University, Seoul 151-742, Korea;

and SungKyunKwan University, Suwon 440-746, Korea

²³*High Energy Accelerator Research Organization (KEK), Tsukuba, Ibaraki 305, Japan*

²⁴*Ernest Orlando Lawrence Berkeley National Laboratory, Berkeley, California 94720*

²⁵*Massachusetts Institute of Technology, Cambridge, Massachusetts 02139*

²⁶*University of Michigan, Ann Arbor, Michigan 48109*

²⁷*Michigan State University, East Lansing, Michigan 48824*

²⁸*University of New Mexico, Albuquerque, New Mexico 87131*

²⁹*Northwestern University, Evanston, Illinois 60208*

³⁰*The Ohio State University, Columbus, Ohio 43210*

³¹*Osaka City University, Osaka 588, Japan*

³²*University of Oxford, Oxford OX1 3RH, United Kingdom*

³³*Universita di Padova, Istituto Nazionale di Fisica Nucleare, Sezione di Padova, I-35131 Padova, Italy*

³⁴*University of Pennsylvania, Philadelphia, Pennsylvania 19104*

³⁵*Istituto Nazionale di Fisica Nucleare, University and Scuola Normale Superiore of Pisa, I-56100 Pisa, Italy*

³⁶*University of Pittsburgh, Pittsburgh, Pennsylvania 15260*

³⁷*Purdue University, West Lafayette, Indiana 47907*

³⁸*University of Rochester, Rochester, New York 14627*

³⁹*Rockefeller University, New York, New York 10021*⁴⁰*Rutgers University, Piscataway, New Jersey 08855*⁴¹*Texas A&M University, College Station, Texas 77843*⁴²*Texas Tech University, Lubbock, Texas 79409*⁴³*Institute of Particle Physics, University of Toronto, Toronto M5S 1A7, Canada*⁴⁴*Istituto Nazionale di Fisica Nucleare, University of Trieste/Udine, Udine, Italy*⁴⁵*University of Tsukuba, Tsukuba, Ibaraki 305, Japan*⁴⁶*Tufts University, Medford, Massachusetts 02155*⁴⁷*Waseda University, Tokyo 169, Japan*⁴⁸*University of Wisconsin, Madison, Wisconsin 53706*⁴⁹*Yale University, New Haven, Connecticut 06520*

(Received 17 May 2002; published 27 December 2002)

The exclusive $\gamma\cancel{E}_T$ signal has a small standard model cross section and is thus a channel sensitive to new physics. This signature is predicted by models with a superlight gravitino or with large extra spatial dimensions. We search for such signals at the Collider Detector at Fermilab, using 87 pb^{-1} of data at $\sqrt{s} = 1.8 \text{ TeV}$, and extract 95% C.L. limits on these processes. A limit of 221 GeV is set on the scale $|F|^{1/2}$ in supersymmetric models. For 4, 6, and 8 extra dimensions, model-dependent limits on the fundamental mass scale M_D of 0.55, 0.58, and 0.60 TeV, respectively, are found. We also specify a “pseudo-model-independent” method of comparing the results to theoretical predictions.

DOI: 10.1103/PhysRevLett.89.281801

PACS numbers: 13.85.Rm, 11.10.Kk, 12.60.Jv, 14.80.-j

Many extensions to the standard model predict the existence of minimally interacting particles, such as the gravitino in supersymmetric models and Kaluza-Klein (KK) modes of the graviton in models with large compact spatial dimensions [1]. Such particles cannot be directly observed in a detector, but their production can be inferred from missing transverse energy (\cancel{E}_T [2]) among the visible particles in a high-energy collision. Photons can be emitted in such hard-scattering processes due to the presence of charged quarks in the $p\bar{p}$ initial state; many models also predict the production of photons from the decay of final-state particles [3]. A search for the $\gamma\cancel{E}_T$ signature thus explores a wide range of models and complements searches in the single jet + \cancel{E}_T channel [4]. Here we present the results of a search in the exclusive $\gamma\cancel{E}_T$ signature, i.e., where only a photon and invisible particles are produced.

The data used for this analysis were collected with the Collider Detector at Fermilab (CDF) during Run 1b of the Tevatron, with an integrated luminosity of $87 \pm 4 \text{ pb}^{-1}$ of $p\bar{p}$ collisions at $\sqrt{s} = 1.8 \text{ TeV}$. The CDF detector has been described in detail elsewhere [5]; subsystems most important to this search are summarized here. A system of time projection chambers around the beam pipe allows the determination of the event vertex position. Surrounding these chambers is the central tracking chamber (CTC), a cylindrical drift chamber inside a 1.4 T superconducting solenoid, which is fully efficient for track reconstruction in the pseudorapidity region $|\eta| < 1.0$ [6]. The central electromagnetic calorimeter (CEM) covers the region $|\eta| < 1.1$. Strip chambers (the CES system) are embedded in the CEM at the depth of the shower maximum to allow the measurement of the two-dimensional transverse profile of electromagnetic showers. The central hadronic calorimeter covers the range

$|\eta| < 1.3$ and is instrumented with time-to-digital converters which associate times to shower signals. The calorimeter modules are arranged in “towers,” with hadronic modules behind the electromagnetic modules, in a projective geometry pointing at the center of the detector. High-energy electromagnetic showers frequently leak from the CEM modules into the hadronic modules behind them; when sufficient leakage occurs timing can be associated with the electromagnetic shower. Outside the calorimeters, drift chambers identify muons in the region $|\eta| < 1.0$.

The CDF three-level trigger system [7] selects events with high- p_T photons during data taking. Level 1 requires a central tower with $E_T^{EM} > 8 \text{ GeV}$ [6]. The Level 2 system forms clusters of towers and then requires the event to pass a logical OR of several triggers, including (a) a loose trigger requiring only an electromagnetic cluster [8] with $E_T^{EM} > 50 \text{ GeV}$ and (b) a trigger requiring $\cancel{E}_T > 35 \text{ GeV}$. Level 3 requires that the photon candidate satisfy $E_T > 50 \text{ GeV}$ and have a CES cluster within the fiducial region [9].

The off-line photon candidate identification (“photon ID”) criteria [9–11] are (a) an electromagnetic cluster in the CEM with $|\eta^\gamma| < 1$ [12], a ratio E^{HAD}/E^{EM} less than $0.055 + 0.00045 \times E^{SUM}$, a centroid within the fiducial region of the CES, and shower evolution measured by the CES consistent with expectation; (b) no second energetic object in the same CES wire chamber as the cluster; (c) at most one CTC track, and none with $p_T > 1 \text{ GeV}$ [13], pointing at the cluster; (d) within a radius of 0.4 in η - ϕ space around the cluster centroid, E_T (summed over towers excluding those in the photon cluster) $< 2 \text{ GeV}$ and a sum of track $p_T < 5 \text{ GeV}$; (e) $E_T^\gamma > 55 \text{ GeV}$ [14]; and (f) an event vertex within 60 cm of the center of the detector along the beam line.

We require $\cancel{E}_T > 45$ GeV. This threshold is lower than the E_T^γ threshold to give full efficiency for signal processes, taking into consideration the \cancel{E}_T resolution and the intrinsic parton p_T in the p and \bar{p} initial states.

Backgrounds to the $\gamma\cancel{E}_T$ signal include: (a) $q\bar{q} \rightarrow Z\gamma \rightarrow \nu\bar{\nu}\gamma$; (b) cosmic ray muons that undergo bremsstrahlung in the CEM but for which no track is found; (c) $W \rightarrow e\nu$ with the electron misidentified as a photon; (d) $W\gamma$ production where the charged lepton in a leptonic W decay is lost; (e) prompt $\gamma\gamma$ production where a photon is lost; and (f) dijet and photon + jet production. The expected number of events from each background source is shown in Table I.

To reject cosmic ray muons, we require a timing signal in the hadronic calorimeter which is in-time with the collision within a window 55 ns wide for at least one tower in the cluster, and no evidence of a muon in the central muon systems within 30° in ϕ of the photon. The efficiency of requiring timing information rises with E_T^γ from 78% at 55 GeV to over 98% above 100 GeV; the timing resolution for photons is on the order of 4 ns. The efficiency of these two cuts is measured with a sample of isolated electrons.

To remove the $W\gamma$ background as well as events in which mismeasurement of jet energy produces fake \cancel{E}_T , we require no jets [8] with $E_T > 15$ GeV, no jets with $E_T > 8$ GeV within 0.5 rad in ϕ of the photon, and no tracks in the event with $p_T > 5$ GeV.

Trigger and background considerations drive the choice of the E_T^γ threshold. The Level 3 trigger becomes fully efficient ($> 99\%$) at 55 GeV. In addition, below 45 GeV the background from $W \rightarrow e\nu$ with a misidentified electron is very large; as the E_T^γ threshold is increased beyond the kinematic limit for electrons from W decay at rest, the W must recoil against another object, and the event is then rejected by the jet and track vetoes.

For an exclusive photon and invisible particle process, the overall efficiency for all cuts is found to vary from 0.45 at $E_T^\gamma = 55$ GeV to 0.56 for $E_T^\gamma > 100$ GeV, with a $\pm 10\%$ uncertainty. The cumulative effect of each cut is shown in Fig. 1. The number of events surviving the photon ID, \cancel{E}_T , cosmic ray rejection, and jet and track

TABLE I. Background sources. The uncertainty in the QCD background is unknown, and this background is not considered when setting limits. The numbers do not total due to rounding.

Cosmic rays	6.3 ± 2.0
$Z\gamma \rightarrow \nu\bar{\nu}\gamma$	3.2 ± 1.0
$W \rightarrow e\nu$	0.9 ± 0.1
Prompt $\gamma\gamma$	0.4 ± 0.1
$W\gamma$	0.3 ± 0.1
Total non-QCD background	11.0 ± 2.2
QCD background	~ 1
Total observed	11

cuts are 15 046, 1475, 94, and 11, respectively. The largest measured difference between E_T^γ and \cancel{E}_T in the 11 events is 8.2 GeV and the mean value of $|E_T^\gamma - \cancel{E}_T|$ is 3.2 GeV, reflecting the detector's good resolution for unclustered energy.

To estimate the number of cosmic ray events in the signal sample, we use the events which have a timing signal outside the in-time window but which pass all other cuts. We then extrapolate into the signal region, assuming a flat distribution in-time [15].

The Monte Carlo simulations of both signal processes and the $Z\gamma$, $W\gamma$, and prompt $\gamma\gamma$ backgrounds use the PYTHIA event generator [16] with the CTEQ5L parton distribution functions (PDFs) [17], followed by a parametrized simulation of the CDF detector. The simulations are then corrected for deficiencies in the detector model and the $\pm 10\%$ efficiency uncertainty applied. We turn off initial state radiation (ISR) to obtain leading-order (LO) cross sections and efficiencies. For the background processes, the resulting cross sections are corrected by the ratio of the LO cross section to the next-to-leading-order "zero-jet" cross section, obtained from theoretical calculations and Monte Carlo estimates. This allows the correct estimation of the acceptance \times efficiency \times cross section ($A\epsilon\sigma$) for the exclusive process. We obtain correction factors of 0.95 ± 0.3 for $Z\gamma$ [18], 0.9 ± 0.2 for $W\gamma$ [19], and 1.0 ± 0.3 for prompt $\gamma\gamma$ [20]; the systematic uncertainties considered are Q^2 choice and acceptance variations due to modeling of ISR in the Monte Carlo simulations. These uncertainties are added in quadrature with the efficiency uncertainty.

The background from $W \rightarrow e\nu$ arises either from hard bremsstrahlung by the electron before it enters the tracking chamber or inefficiency in the track reconstruction.

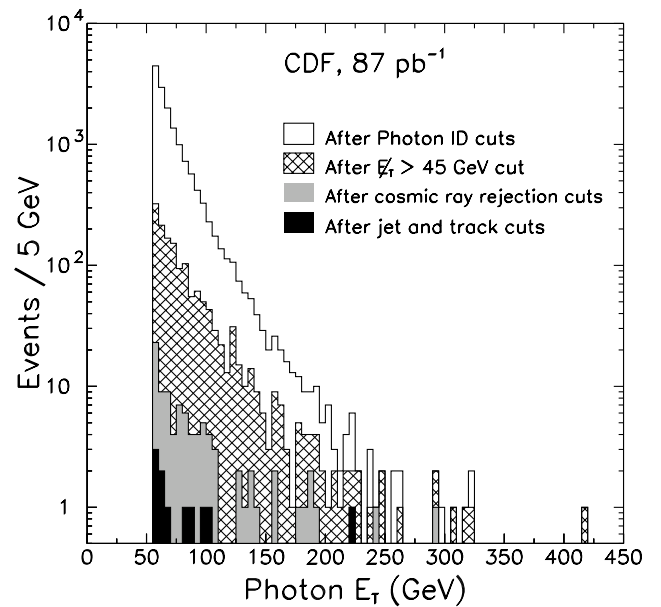


FIG. 1. Photon E_T spectrum after each stage of cuts.

As a radiated photon tends to be collinear with the electron, the E_T of the identified electromagnetic object will be close to the initial energy of the electron. We estimate the ratio \mathcal{P} between the number of electrons faking photons and the number of electrons passing standard electron identification cuts [9] in the region $|\eta^e| < 1$, by assuming that “ $e\gamma$ ” events with invariant masses within 10 GeV of the Z^0 mass are actually $Z^0 \rightarrow ee$ events. We obtain $\mathcal{P} = (0.8 \pm 0.1)\%$. The background estimate is \mathcal{P} times the number of $W \rightarrow e\nu$ events that have $|\eta^e| < 1$, $E_T^e > 55$ GeV, $\cancel{E}_T > 45$ GeV, and pass the jet and track vetoes (discounting the electron track).

We have investigated QCD backgrounds which involve the mismeasurement of jet energy leading to apparent \cancel{E}_T or misidentification of a jet as a photon. The most likely contributors to fakes are events with one high-energy object and many low-energy jets. With the \cancel{E}_T , jet, and track requirements, these events are rare. To estimate these backgrounds one must use data; however, all control samples have small statistics and estimates range from 0.1 to 2 events. We take the conservative approach of not including this background source in the total background used in the limit calculations. This can only make the limits less stringent [21].

We study two hypothetical signal processes in detail. One is predicted by a supersymmetric model and the other by a model with large compact extra dimensions.

The first process ($q\bar{q} \rightarrow \tilde{G}\tilde{G}\gamma$) is described in [22]. It presumes that the gravitino \tilde{G} is the lightest supersymmetric particle, with the other superpartners too heavy to produce at the Tevatron. Since the gravitino coupling is very small, being able to produce other supersymmetric particles increases the cross section; we therefore set an absolute lower limit on the gravitino mass $m_{3/2}$ or, equivalently, the supersymmetry breaking scale $|F|^{1/2}$ (the two are related by $|F| = \sqrt{3}m_{3/2}M_P$, with M_P being the Planck mass). The cross section for this process scales as $1/|F|^4$; the kinematic distributions are independent of $|F|$.

The second process ($q\bar{q} \rightarrow \gamma G_{KK}$) is described in [23]: n extra spatial dimensions are assumed to be compactified with radius R . The fundamental mass scale M_D and R are related to n and Newton’s constant by $G_N^{-1} = 8\pi R^n M_D^{2+n}$ [24]. The standard model fields propagate only on a $3+1$ dimensional subspace, while gravitons propagate in the whole space. The graviton modes which propagate in the extra dimensions appear to four-dimensional observers as massive states of the graviton. A large value of R results in a large phase space for graviton production, canceling the weakness of the coupling to standard model fields. For a given n , the cross section scales as $1/M_D^{n+2}$; for fixed n , the kinematic distributions are independent of M_D .

Collisions at the Tevatron occur at sufficiently high values of the parton center-of-mass energies ($\sqrt{\hat{s}}$) that we must consider the behavior of the differential cross

section for collisions with $\sqrt{\hat{s}} > M_D$. We assume that the effective theory is valid for $\sqrt{\hat{s}} \lesssim 2M_D$. Our limits are sensitive to this choice as explained below.

The two signal processes are simulated with modified versions of PYTHIA. The $q\bar{q} \rightarrow \tilde{G}\tilde{G}\gamma$ process is simulated with $|F|^{1/2} = 100$ GeV, and the $q\bar{q} \rightarrow \gamma G_{KK}$ process is simulated with $M_D = 1$ TeV for $n = 4, 6$, and 8 extra dimensions.

We obtain estimates of three sources of theoretical systematic uncertainty in the cross section and acceptance predictions by varying Q^2 by a factor of 4 up and down, by using the GRV98 LO PDFs [25], and by turning the modeling of ISR on and off. The uncertainty due to ISR includes order- α_s effects and acceptance changes due to the jet and track vetoes. For $q\bar{q} \rightarrow \tilde{G}\tilde{G}\gamma$, the dominant uncertainty is the Q^2 choice ($^{+26}_{-18}\%$), followed by ISR ($\pm 14\%$) and PDF choice ($\pm 10\%$). For $q\bar{q} \rightarrow \gamma G_{KK}$, the dominant uncertainty comes from ISR ($\pm 34\%$), followed by Q^2 choice ($^{+18}_{-16}\%$) and PDF choice ($\pm 8\%$). The overall uncertainty in $A\epsilon\sigma$ for the $q\bar{q} \rightarrow \tilde{G}\tilde{G}\gamma$ process, which includes the $\pm 10\%$ efficiency uncertainty, is $^{+33}_{-27}\%$. For $q\bar{q} \rightarrow \gamma G_{KK}$, the corresponding figure is $\pm 40\%$.

The method we use to set limits is outlined in [26]. We find the following limits at 95% C.L.: for the supersymmetric model, $|F|^{1/2} \geq 221$ GeV (equivalently, $m_{3/2} \geq 1.17 \times 10^{-5}$ eV); for large extra dimensions, $M_D \geq 0.55, 0.58$, and 0.60 TeV for $n = 4, 6$, and 8 extra dimensions (equivalently, $R \leq 24$ pm, 55 fm, and 2.6 fm, respectively). Similar limits on $|F|^{1/2}$ have previously been set in Refs. [4,27–30]; limits on M_D in the real graviton emission channel have been set in Refs. [27–30].

The kinematic region in E_T^γ and $\sqrt{\hat{s}}$ explored here is very different from that probed at LEP, and the limits on M_D are more dependent on the behavior of the cross section for $\sqrt{\hat{s}} > M_D$. For illustration, we have evaluated the limits using the prescription of suppressing the cross section by a factor of M_D^4/\hat{s}^2 above M_D [31]. These limits are set without including the 40% theoretical uncertainty. The limits decrease by between 0.01 and 0.05 TeV [32].

The results of this analysis can be presented in a “pseudo-model-independent” manner. In both the above models, the uncertainties in the predicted numbers of signal events have been dominated by theoretical factors. It can be useful to derive a limit which considers only the uncertainties in the detector simulation of the processes and so can easily be compared across models [10] (keeping in mind that such a limit is not a substitute for the rigorous extraction of a limit noting theoretical uncertainties). To obtain this limit, we compute a 95% C.L. upper limit on the number of events from new physics that would be detected, using only the $\pm 10\%$ uncertainty in efficiency as the uncertainty in the $A\epsilon\sigma$ for the new process. This limit is 9.8 events, which for this integrated luminosity corresponds to a cross section of 112 fb.

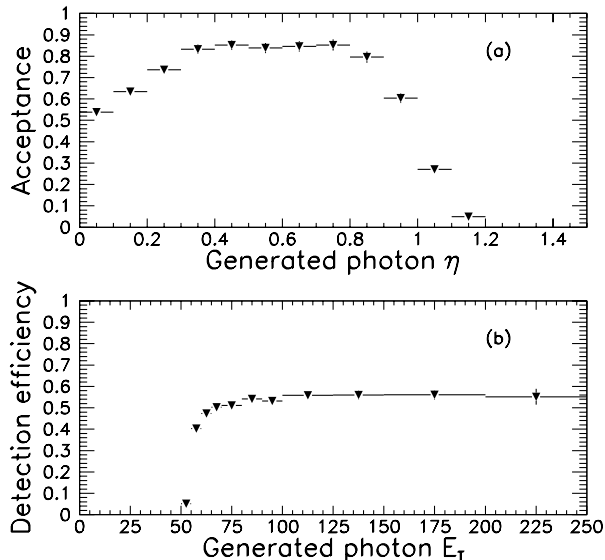


FIG. 2. Plots of (a) acceptance vs η^γ and (b) efficiency vs E_T^γ for the analysis selection. These plots are valid for any exclusive photon and invisible particle process. The error bars are statistical only. The falloff in acceptance at $|\eta| \approx 0$ and $|\eta| \approx 1$ is due to the folding of the fiducial region of the calorimeter with the longitudinal spread ($\sigma \approx 30$ cm) of the $p\bar{p}$ collisions.

The plots in Fig. 2 allow a comparison of models to the $A\epsilon\sigma$ limit. These curves are obtained by studying the acceptance and efficiency curves for simulated events and correcting for deficiencies in the detector simulation. These plots are valid for both the $\tilde{G}\tilde{G}\gamma$ and γG_{KK} processes studied above, and for any process producing an exclusive photon and invisible particle signature. One can estimate $A\epsilon\sigma$ for such a process by convolving the theoretical photon η and E_T spectra with the acceptance and efficiency curves.

In conclusion, we have performed a search for new physics in the exclusive $\gamma\cancel{E}_T$ channel. We have found no departure from the expected standard model cross section and have set limits on two specific models of new physics, one a supersymmetric model in which the photon is produced in association with two gravitinos, the second a model with large extra dimensions in which the photon is produced in association with a KK mode of the graviton. We have also presented the limit in a “pseudo-model-independent” manner.

We thank the Fermilab staff and the technical staffs of the participating institutions for their vital contributions. We would also like to thank J. Lykken, K. Matchev, and D. Rainwater for their help. This work was supported by the U.S. Department of Energy and National Science Foundation; the Italian Istituto Nazionale di Fisica Nucleare; the Ministry of Education, Culture, Sports, Science, and Technology of Japan; the Natural Sciences and Engineering Research Council of Canada; the National Science Council of the Republic of China; the

Swiss National Science Foundation; the A. P. Sloan Foundation; the Bundesministerium für Bildung und Forschung, Germany; the Korea Research Foundation and the Korea Science and Engineering Foundation (KoSEF); and the Comision Interministerial de Ciencia y Tecnologia, Spain.

*Present address: University of California, Santa Barbara, California 93106

- [1] N. Arkani-Hamed, S. Dimopoulos, and G. Dvali, *Phys. Lett. B* **429**, 263 (1998).
- [2] $E_T \equiv E \sin\theta$, where θ is the polar angle of the object measured relative to the event vertex. \cancel{E}_T is defined as the magnitude of the vector sum of E_T over all objects in the event.
- [3] Two examples of such models are S. Ambrosanio *et al.*, *Phys. Rev. Lett.* **76**, 3498 (1996); B. C. Allanach *et al.*, hep-ph/0112321.
- [4] T. Affolder *et al.*, *Phys. Rev. Lett.* **85**, 1378 (2000).
- [5] F. Abe *et al.*, *Nucl. Instrum. Methods Phys. Res., Sect. A* **271**, 387 (1988).
- [6] The CDF coordinate system is right-handed with the x axis horizontal and out of the Tevatron ring, the y axis up, and the z axis along the proton beam; ϕ is the azimuthal angle. The pseudorapidity $\eta \equiv -\ln[\tan(\theta/2)]$, where θ is the polar angle; the η regions for detector components are defined with respect to the center of the detector.
- [7] D. Amidei *et al.*, *Nucl. Instrum. Methods Phys. Res., Sect. A* **350**, 73 (1994).
- [8] F. Abe *et al.*, *Phys. Rev. D* **50**, 2966 (1994).
- [9] D. Acosta *et al.*, *Phys. Rev. D* **66**, 012004 (2002).
- [10] T. Affolder *et al.*, *Phys. Rev. D* **65**, 052006 (2002).
- [11] T. Affolder *et al.*, *Phys. Rev. D* **59**, 092002 (1999).
- [12] Here η^γ is defined with respect to the center of the detector.
- [13] We use the convention that “momentum” refers to pc and “mass” to mc^2 , so that energy, momentum, and mass are all measured in GeV.
- [14] The E_T and \cancel{E}_T values used in the off-line selections are corrected values (see Ref. [8]).
- [15] The calorimeter response is the same in-time and out-of-time; however, the CTC will fail to find out-of-time tracks. A CEM cluster will not be identified as a photon if it has an energetic track pointing at it, which is more likely if the cosmic ray occurs in-time. We have searched for such events (a track originating far from an interaction vertex in z , with p_T not matching calorimeter E_T , and/or large impact parameter) and find none. Any residual effect is accounted for in the quoted systematic uncertainty in this background.
- [16] T. Sjöstrand *et al.*, *Comput. Phys. Commun.* **135**, 238 (2001), we use version 6.156.
- [17] H. Lai *et al.*, *Phys. Rev. D* **55**, 1280 (1997).
- [18] U. Baur, T. Han, and J. Ohnemus, *Phys. Rev. D* **57**, 2823 (1998).

- [19] U. Baur, T. Han, and J. Ohnemus, Phys. Rev. D **48**, 5140 (1993).
- [20] B. Bailey, J. Ohnemus, and J. F. Owens, Phys. Rev. D **46**, 2018 (1992).
- [21] Estimates of backgrounds with small central values but large uncertainties are necessarily highly asymmetric, as a background cannot be less than zero. During the limit-setting procedure, this would produce artificially high limits.
- [22] A. Brignole, F. Feruglio, M.L. Mangano, and F. Zwirner, Nucl. Phys. **B526**, 136 (1998); **B582**, 759 (E) (2000).
- [23] G. F. Giudice, R. Rattazzi, and J. D. Wells, Nucl. Phys. **B544**, 3 (1999), updated in hep-ph/9811291 v2.
- [24] This is in the convention of Giudice *et al.*; other authors replace 8π by other values.
- [25] M. Glück, E. Reya, and A. Vogt, Eur. Phys. J. C **5**, 461 (1998).
- [26] J. Conway, in *Proceedings of the 1st Workshop on Confidence Limits, 2000* (CERN-2000-005).
- [27] A. Heister *et al.*, Report No. CERN-EP-2002-033, 2002 [Eur. Phys. J. C (to be published)].
- [28] P. Abreu *et al.*, Eur. Phys. J. C **17**, 53 (2000).
- [29] M. Acciarri *et al.*, Phys. Lett. B **470**, 268 (1999).
- [30] G. Abbiendi *et al.*, Eur. Phys. J. C **18**, 253 (2000).
- [31] I. Hinchliffe and L. Vacavant, hep-ex/0005033.
- [32] The results are $M_D \geq 0.54, 0.55,$ and 0.55 TeV for $n = 4, 6,$ and $8,$ respectively.